

Chitosan stabilised nanozero-valent iron for the catalytic reduction of p-nitrophenol

Hongfei Lu, Xueliang Qiao, Wei Wang, Fatang Tan, Zunqi Xiao, Jianguo Chen

State Key Laboratory of Material Processing and Die & Mould Technology, Huazhong University of Science and Technology, Wuhan 430074, People's Republic of China

E-mail: hflu2011@163.com

Published in Micro & Nano Letters; Received on 16th March 2014; Revised on 22nd May 2014; Accepted on 4th June 2014

Chitosan stabilised nanozero-valent iron (CNZVI) is proposed as a catalyst because of its simple preparation and high activity. The catalytic activity of CNZVI was investigated using the reduction reaction of p-nitrophenol (p-NP) by NaBH_4 . The result indicated that CNZVI possessed good catalytic activity, and the rate constant (k) was $2.45 \times 10^{-3} \text{ s}^{-1}$. In addition, CNZVI can be easily separated by an external magnetic field from aqueous solution, and it could also be repeatedly applied for the reduction of p-NP for at least five successive cycles with stable catalytic activity. All of these results suggest that CNZVI could be used as an excellent catalyst for the catalytic reduction of p-NP by NaBH_4 .

1. Introduction: p-Aminophenol (p-AP) is an important intermediate for the manufacture of analgesic and antipyretic drugs, which can be synthesised by the reduction of p-nitrophenol (p-NP) [1–3]. Conventionally, the reduction of p-NP to p-AP has been carried out using an iron-acid reducing agent. A major drawback of this method is the generation of large amounts of Fe–FeO sludge, which cannot be reused and causes severe disposal problems [4]. The direct catalytic hydrogenation is also an effective route for the reduction of p-NP. However, the application of this method is restricted, because it needs to be carried out under the conditions of high temperature and pressure [1, 5, 6]. With increasing interest in environmental protection and safe operating, the reduction of p-NP by NaBH_4 using metal nanoparticles as catalysts is an attractive method, since the reaction can be carried out in the aqueous solution.

Nanoparticles have been investigated extensively in recent years because of their particular physical and chemical properties [7]. Metal particles with size in the nanometre regime have higher Fermi potential, which leads to the lowering of the reduction potential value, and hence metal nanoparticles can function as a catalyst for many electron-transfer reactions [8]. In previous studies, several metal nanoparticles, such as Au nanoparticles [9, 10], Ag nanocomposite [11–13] and bimetallic Pt–Ni nanoparticles [14], have been used as catalysts in the reduction reaction of p-NP by NaBH_4 . However, all of these catalysts are noble metals in such reduction reactions, which will lead to an increase of the cost of production. There were also some reports about using nanosized transition metals, such as Ni, Co and NiCo_2O_4 , as catalysts in the reduction reaction of p-NP by NaBH_4 [15–18]. As far as we know, the catalytic performance of nanozero-valent iron (NZVI) in such a reduction reaction was seldom investigated.

In the work reported in this Letter, chitosan stabilised NZVI (CNZVI) was synthesised by a simple chemical reduction method. The textural properties of CNZVI were characterised by Fourier transform infrared spectra (FTIR), X-ray diffraction (XRD) and transmission electron microscopy (TEM). The catalytic activity of CNZVI was investigated by virtue of the reduction reaction of p-NP by NaBH_4 , and the reduction reaction was monitored using a UV–vis spectrometer. The effects of the amount of CNZVI and the reaction temperature on the reduction reaction of p-NP were investigated. Furthermore, the reusability of CNZVI was also explored.

2. Experimental details

2.1. Materials: All chemicals were analytical grade reagents and were used without further purification. Ferrous sulphate

heptahydrate ($\text{FeSO}_4 \cdot 7\text{H}_2\text{O}$) 99%, sodium borohydride (NaBH_4) 96%, chitosan flakes (80–95% deacetylation), absolute ethanol, acetone and p-NP were purchased from the Sinopharm Chemical Reagent Co. Ltd. The water that was used was doubly distilled water.

2.2. Synthesis of CNZVI: CNZVI was synthesised under an argon atmosphere. Firstly, 10 mmol of $\text{FeSO}_4 \cdot 7\text{H}_2\text{O}$ was added to 50 ml of chitosan aqueous solution (0.5%). Secondly, 50 ml of aqueous solution containing 30 mmol of NaBH_4 was added dropwise into the above solution under stirring at room temperature. Finally, the slurry was separated by magnetism and washed three times with deoxygenated water, absolute ethanol and acetone, respectively. CNZVI was dried under vacuum conditions and preserved under an argon atmosphere. The synthesis of bare NZVI was similar to CNZVI but without chitosan.

2.3. Characterisation of CNZVI: CNZVI was characterised by TEM (TEM, JEOL JEM-100CXII with an accelerating voltage of 100 kV), XRD (XRD, Philips X'Pert PRO with $\text{Cu-K}\alpha$ radiation and an accelerating voltage of 40 kV and an emission current of 40 mA) and FTIR spectra (FTIR, Bruker VERTEX 70).

2.4. Catalytic activity test: To evaluate the catalytic performance of CNZVI catalyst, 200 ml of $2.06 \times 10^{-4} \text{ mol l}^{-1}$ aqueous solution of p-NP was added into an Erlenmeyer flask. Then, $4.12 \times 10^{-3} \text{ mol}$ of NaBH_4 was added into the flask. To the mixture, 0.2 g of CNZVI catalyst was added. The mixture solution was shaken at room temperature. 1 ml of the sample was taken out at various time intervals and measured by a UV–vis spectrometer. For recycling experiments, CNZVI catalyst was collected by an external magnetic field and washed three times with distilled water, and then reused.

3. Results and discussion

3.1. Characterisation of CNZVI: To identify possible interactions between chitosan and NZVI particles, FTIR spectra were obtained for chitosan and CNZVI. The results are shown in Fig. 1a. The characteristic peaks at 1653, 1390 and 1087 cm^{-1} for chitosan contributed to N–H bending vibration, C–O stretching of primary alcoholic group and C–O stretching vibration, respectively [19]. The FTIR spectrum for CNZVI showed a shift of the peaks at 1653–1623, 1390–1335 and $1087\text{--}1028 \text{ cm}^{-1}$. The results revealed that chitosan was adsorbed on the surface of the NZVI nanoparticles [20]. The XRD patterns of bare NZVI and CNZVI are shown in Fig. 1b. As can be

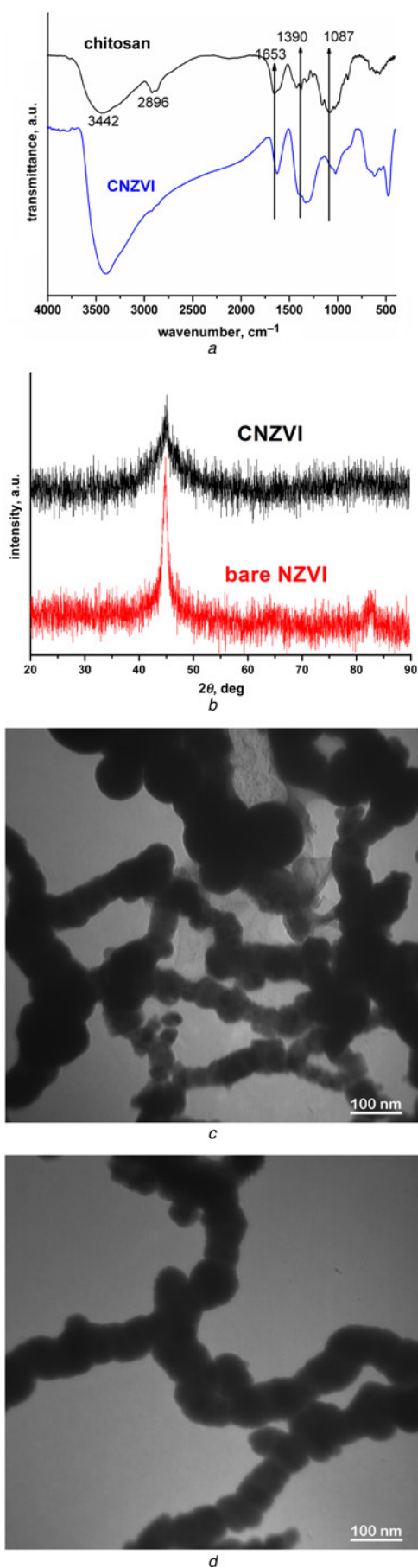


Figure 1 IR spectra of chitosan and CNZVI (Fig. 1a), XRD patterns of bare NZVI and CNZVI (Fig. 1b), TEM image of bare NZVI (Fig. 1c), and TEM image of CNZVI (Fig. 1d)

Table 1 Reaction rate constants (k , min⁻¹) and linear correlation coefficients (R) of the reduction reactions at different concentration ratios of NaBH₄ to p-NP

[NaBH ₄]/[p-NP]	20	30	40	60	80	100
k , min ⁻¹	0.0928	0.1221	0.1452	0.1458	0.1461	0.1468
R	0.9764	0.9801	0.9849	0.9835	0.9904	0.9918

observed, the main formation of bare NZVI and CNZVI was in the zero-valent state as confirmed by the characteristic diffraction peak at $2\theta = 44.7^\circ$ [21]. Meanwhile, the diffraction peak at $2\theta = 44.7^\circ$ of CNZVI was broadened in contrast to that of bare NZVI, which also indicated that NZVI particles were stabilised by chitosan and the iron particles were nanometre in size [22, 23]. Figs. 1c and d show the TEM images of bare NZVI and CNZVI, respectively. It was found that the bare NZVI particles formed short chains of beads because of the strong van der Waals attraction as well as the magnetic interactions between the primary particles [24]. CNZVI particles did not appear as discrete nanoscale particles, but formed long chain-like aggregates. This type of aggregation may be attributed to the encapsulated function of chitosan.

3.2. Catalysis study: To investigate the catalytic properties of CNZVI, the reduction reaction of p-NP by an excess of NaBH₄ as a model reaction was chosen. The mixture solution of p-NP and NaBH₄ has a characteristic absorption peak at 400 nm in the UV-vis spectrum, which was assumed to be from the p-NP anion because of NaBH₄ alkaline solutions [25]. In the absence of CNZVI catalyst, the intensity of the absorption peak at 400 nm did not change significantly even after several days, which implies that p-NP cannot be reduced by NaBH₄. It also reveals that no reduction of p-NP occurred without CNZVI catalyst. Then, the reduction reaction was tested in the presence of 0.20 g of CNZVI catalyst by using 20-, 30-, 40-, 60-, 80- and 100-fold more NaBH₄ than p-NP, respectively. Since the concentration of NaBH₄ was in great excess compared with p-NP, its concentration can be considered as constant during the reaction. Therefore these reactions can be treated as a pseudo-first-order reaction [26].

The reaction rate constants (k) and the correlation coefficients (R) for the reactions were calculated according to (1) and are listed in Table 1.

$$\ln c = kt + b \quad (1)$$

where c is the concentration of p-NP at any time t , k (min⁻¹) is the

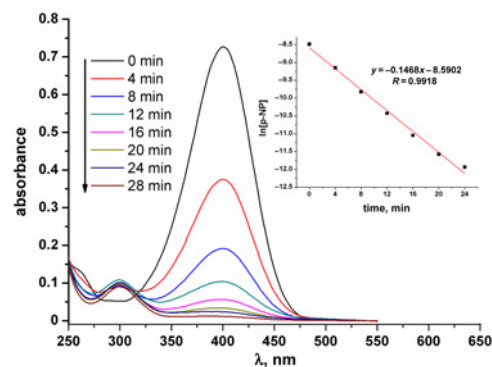


Figure 2 UV-vis spectra of the reduction reaction of p-NP catalysed by CNZVI in aqueous solution of NaBH₄ (experimental condition: solution volume = 200 ml, [NaBH₄]/[p-NP] = 100, CNZVI = 0.20 g, $T = 298$ K and 250 rpm)

rate constant of pseudo-first-order kinetics, t (min) is the reaction time and b is a constant.

As shown in Table 1, the reaction rate constant (k) was increased and the linear correlation coefficient (R) was much better when increasing the amount of NaBH_4 . To better ensure that the reaction complied with the pseudo-first-order kinetics, 100-fold excess NaBH_4 was used for the reduction reaction of p-NP.

Fig. 2 as a typical spectrum displayed the reduction reaction of p-NP at 100-fold excess NaBH_4 and in the presence of 0.20 g of CNZVI catalyst. It can be seen that the intensity of the absorption peak at 400 nm was gradually decreased; meanwhile, a new peak at 300 nm for p-AP was observed as the reaction progressed [14, 15, 27]. After half an hour, the absorption peak at 400 nm almost disappeared, which indicated that the reaction was complete. These results suggested that the CNZVI indeed possessed excellent catalytic activity to the reduction of p-NP. Additionally, the plot of $\ln[\text{p-NP}]$ against time showed a good linear correlation ($R = 0.9918$), as shown in the inserted pattern in Fig. 2, which confirmed that the reduction reaction complied with the pseudo-first-order kinetics. The rate constant (k) is $2.45 \times 10^{-3} \text{ s}^{-1}$, which can be obtained from Fig. 2. This value is higher than the reported value for Ni nanoparticles [28]. However, the rate constant value is lower than that of Ag nanoparticles ($k = 2.78 \times 10^{-3} \text{ s}^{-1}$) and Au@Ag nanoparticles ($k = 4.97 \times 10^{-3} \text{ s}^{-1}$) [29, 30]. Although the catalytic activity of CNZVI is lower than that of some materials, the cost of CNZVI is lower than noble metal catalysts. Therefore CNZVI could be used as a catalyst in such reduction reactions.

As a control experiment, the catalytic activity of bare NZVI was also investigated under the same conditions of 100-fold excess NaBH_4 and 0.20 g of bare NZVI catalyst. The value of the rate constant is $1.63 \times 10^{-3} \text{ s}^{-1}$, which is lower than that of CNZVI. It is because bare NZVI particles are prone to form aggregations and the surface of bare NZVI particles can be easily oxidised by air.

As is known, the catalytic reduction of p-NP by NaBH_4 in the presence of a catalyst occurs via the relaying of electrons from the electron donor (BH_4^-) to the acceptor (p-NP). In aqueous medium, BH_4^- was adsorbed on the surface of the catalyst. The hydrogen atom which was formed from hydride, after electron transfer to the CNZVI, attacked p-NP molecules to reduce them. This electron transfer induced hydrogenation of p-NP occurred spontaneously [11]. Moreover, the liberation of hydrogen by the hydrolysis reaction of NaBH_4 and water could be accelerated because of the presence of a catalyst [31].

3.3. Effect of the amount of CNZVI catalyst: Fig. 3a shows the plots of the concentration of p-NP against time at different amounts of CNZVI catalyst. It was observed that the concentration of p-NP gradually decreased and the reduction rate was increased with increasing the amount of CNZVI catalyst. In addition, the plots of $\ln[\text{p-NP}]$ against time yielded good linear correlations as indicated in Fig. 3b, revealing that the reduction of p-NP catalysed by CNZVI catalyst in the presence of NaBH_4 followed the pseudo-first-order kinetics. These results demonstrated that the reaction rate of p-NP could be influenced by the amount of CNZVI catalyst, which was similar to the reports of previous studies [32–34].

3.4. Effect of the reaction temperature: Since the temperature is a very important factor in the catalytic reaction, the catalytic reduction of p-NP by NaBH_4 was also studied at different temperatures in the range of 293–308 K. Fig. 4a shows the plots of $\ln[\text{p-NP}]$ against time at different temperatures. It can be observed that the reaction rate was increased with increasing reaction temperature. Furthermore, we also discussed the apparent activation energy (E_a) based on the linear fitting of $\ln k$ against

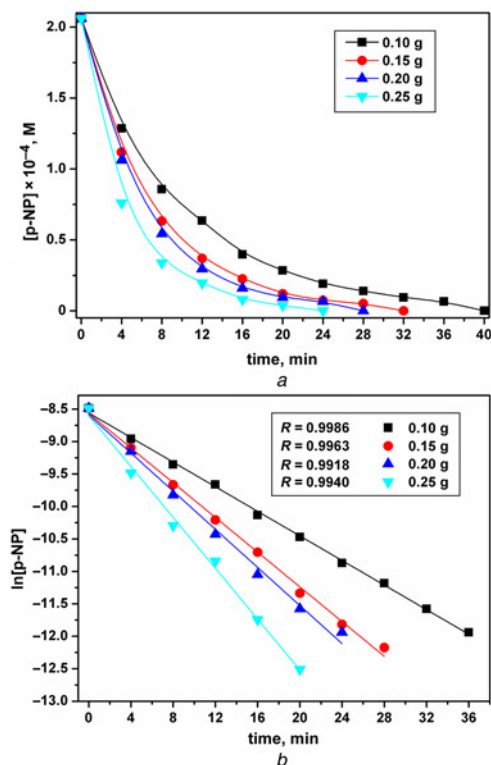


Figure 3 Plots of concentration of p-NP against time for reduction of p-NP by NaBH_4 at different amounts of CNZVI catalyst (Fig. 3a), and plots of $\ln[\text{p-NP}]$ against time (experimental conditions: solution volume = 200 ml, $[\text{NaBH}_4]/[\text{p-NP}] = 100$, $T = 298 \text{ K}$ and 250 rpm) (Fig. 3b)

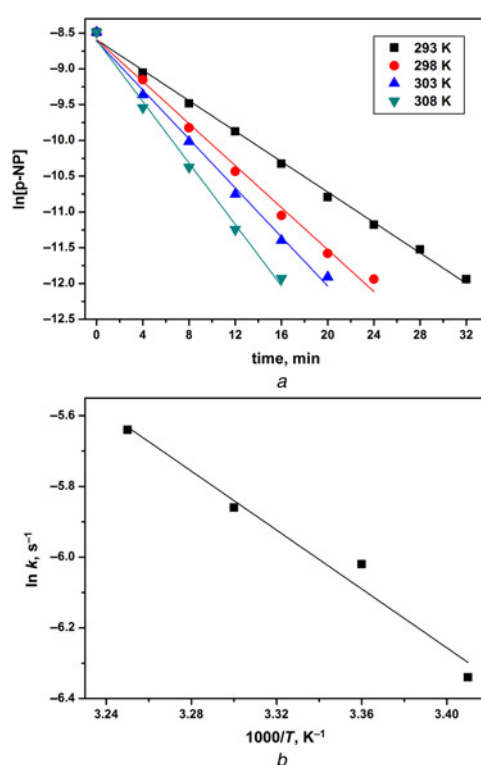


Figure 4 Plots of $\ln[\text{p-NP}]$ against time at different temperatures (experimental conditions: solution volume = 200 ml, $[\text{NaBH}_4]/[\text{p-NP}] = 100$, CNZVI = 0.20 g and 250 rpm) (Fig. 4a), and Arrhenius plot for reduction of p-NP at different temperatures based on data in Fig. 4a (Fig. 4b)

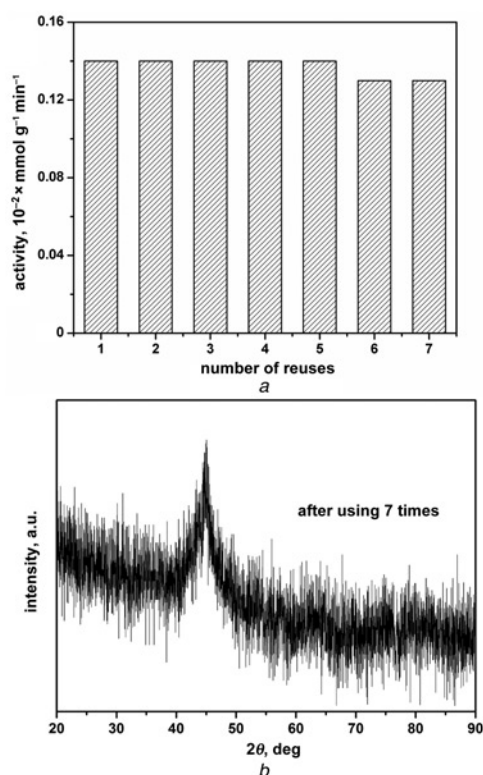


Figure 5 Reusability of CNZVI catalyst for reduction of p-NP by NaBH₄ (experimental conditions: solution volume = 200 ml, [NaBH₄]/[p-NP] = 100, CNZVI = 0.20 g, T = 298 K and 250 rpm) (Fig. 5a), and XRD pattern of CNZVI after using seven times (Fig. 5b)

1000/T (Fig. 4b) and the Arrhenius equation

$$\ln k = \ln A - E_a/RT$$

From the slope of Fig. 4b, the apparent activation energy E_a was calculated to be 34.62 kJ mol⁻¹ or 8.27 kcal mol⁻¹. That is to say, the E_a lies within 2–10 kcal mol⁻¹, which suggests that the p-NP reduction in this case occurs via surface catalysis [35].

3.5. Reusability of CNZVI catalyst: The as-prepared CNZVI catalyst shows both catalytic and magnetic properties which can be easily recycled by an external magnet after the catalytic reaction. The reusability of CNZVI catalyst in the reduction of p-NP is shown in Fig. 5a. The catalyst can be successfully recycled and reused at least five times with stable catalytic activity. It could be suggested that CNZVI catalyst was not deactivated or poisoned during the catalytic or separation processes. Moreover, compared with Fig. 1b, the XRD pattern of CNZVI nanoparticles did not change significantly after seven cycles of catalytic reactions, as shown in Fig. 5b. This showed that CNZVI nanoparticles were stable, and were still in the zero-valent state as confirmed by the characteristic diffraction peak at $2\theta = 44.7^\circ$ [21]. These results also indicated that CNZVI was stable and could be used as an excellent catalyst in the catalytic reaction of p-NP by NaBH₄.

4. Conclusion: This investigation demonstrated that CNZVI was an effective catalyst for the catalytic reduction of p-NP by NaBH₄ at room temperature. Moreover, CNZVI catalyst showed good separability and reusability in successive cycles of catalytic reaction. The reaction rate increased at higher temperatures and higher amounts of CNZVI catalyst, and the reduction reaction of p-NP by excess NaBH₄ followed pseudo-first-order kinetics.

Overall, this work may be useful in developing an environment-friendly, high activity, low cost and simple preparing catalyst for the reduction of p-NP by NaBH₄ in the aqueous solution under mild conditions.

5. Acknowledgments: The authors thank the Analysis and Test Center of HUST (Huazhong University of Science and Technology) for providing all the required facilities to carry out the experiments.

6 References

- [1] Vaidya M.J., Kulkarni S.M., Chaudhari R.V.: 'Synthesis of P-aminophenol by catalytic hydrogenation of P-nitrophenol', *Org. Process Res. Dev.*, 2003, **7**, (2), pp. 202–208
- [2] Du Y., Chen H., Chen R., Xu N.: 'Synthesis of P-aminophenol from P-nitrophenol over nano-sized nickel catalysts', *Appl. Catal. A, Gen.*, 2004, **277**, (1), pp. 259–264
- [3] Pan L., Li L., Chen Y.: 'Synthesis of Ag/Cu₂O hybrids and their photocatalytic degradation treatment of P-nitrophenol', *Micro Nano Lett.*, 2011, **6**, (12), pp. 1019–1022
- [4] Rao P., Mak M.S., Liu T., Lai K.C., Lo I.: 'Effects of humic acid on arsenic (V) removal by zero-valent iron from groundwater with special references to corrosion products analyses', *Chemosphere*, 2009, **75**, (2), pp. 156–162
- [5] Rode C., Vaidya M., Chaudhari R.: 'Synthesis of P-aminophenol by catalytic hydrogenation of nitrobenzene', *Org. Process Res. Dev.*, 1999, **3**, (6), pp. 465–470
- [6] Gkizis P.L., Stratakis M., Lykakis I.N.: 'Catalytic activation of hydrazine hydrate by gold nanoparticles: chemoselective reduction of nitro compounds into amines', *Catal. Commun.*, 2013, **36**, (5), pp. 48–51
- [7] El-Sayed M.A.: 'Small is different: shape-, size-, and composition-dependent properties of some colloidal semiconductor nanocrystals', *Acc. Chem. Res.*, 2004, **37**, (5), pp. 326–333
- [8] Pradhan N., Pal A., Pal T.: 'Catalytic reduction of aromatic nitro compounds by coinage metal nanoparticles', *Langmuir*, 2001, **17**, (5), pp. 1800–1802
- [9] Chang Y.-C., Chen D.-H.: 'Catalytic reduction of 4-nitrophenol by magnetically recoverable Au nanocatalyst', *J. Hazard. Mater.*, 2009, **165**, (1), pp. 664–669
- [10] Gupta V.K., Atar N., Yola M.L., Üstündağ Z., Uzun L.: 'A novel magnetic Fe@Au core-shell nanoparticles anchored graphene oxide recyclable nanocatalyst for the reduction of nitrophenol compounds', *Water Res.*, 2014, **48**, pp. 210–217
- [11] Naik B., Hazra S., Prasad V.S., Ghosh N.N.: 'Synthesis of Ag nanoparticles within the pores of Sba-15: an efficient catalyst for reduction of 4-nitrophenol', *Catal. Commun.*, 2011, **12**, (12), pp. 1104–1108
- [12] Zhang W., Tan F., Wang W., Qiu X., Qiao X., Chen J.: 'Facile, template-free synthesis of silver nanodendrites with high catalytic activity for the reduction of P-nitrophenol', *J. Hazard. Mater.*, 2012, **217**, pp. 36–42
- [13] Du X., He J., Zhu J., Sun L., An S.: 'Ag-deposited silica-coated Fe₃O₄ magnetic nanoparticles catalyzed reduction of P-nitrophenol', *Appl. Surf. Sci.*, 2012, **258**, (7), pp. 2717–2723
- [14] Ghosh S.K., Mandal M., Kundu S., Nath S., Pal T.: 'Bimetallic Pt–Ni nanoparticles can catalyze reduction of aromatic nitro compounds by sodium borohydride in aqueous solution', *Appl. Catal. A, Gen.*, 2004, **268**, (1), pp. 61–66
- [15] Sahiner N., Ozay H., Ozay O., Aktas N.: 'A soft hydrogel reactor for cobalt nanoparticle preparation and use in the reduction of nitrophenols', *Appl. Catal. B, Environ.*, 2010, **101**, (1), pp. 137–143
- [16] Swathi T., Buvaneswari G.: 'Application of NiCo₂O₄ as a catalyst in the conversion of P-nitrophenol to P-aminophenol', *Mater. Lett.*, 2008, **62**, (23), pp. 3900–3902
- [17] Wang A., Yin H., Lu H., Xue J., Ren M., Jiang T.: 'Catalytic activity of nickel nanoparticles in hydrogenation of P-nitrophenol to P-aminophenol', *Catal. Commun.*, 2009, **10**, (15), pp. 2060–2064
- [18] Pan L., Li L., Chen Y.: 'Synthesis and electrocatalytic properties for P-nitrophenol reduction of nano-scaled M₂O₄ (M = Fe, Co) products with different shapes', *Micro Nano Lett.*, 2012, **7**, (5), pp. 480–484
- [19] Wan Y., Wu H., Yu A., Wen D.: 'Biodegradable polylactide/chitosan blend membranes', *Biomacromolecules*, 2006, **7**, (4), pp. 1362–1372
- [20] Liang Y.-Y., Zhang L.-M.: 'Bioconjugation of papain on superparamagnetic nanoparticles decorated with carboxymethylated chitosan', *Biomacromolecules*, 2007, **8**, (5), pp. 1480–1486

- [21] Kanel S.R., Manning B., Charlet L., Choi H.: 'Removal of arsenic (Iii) from groundwater by nanoscale zero-valent iron', *Environ. Sci. Technol.*, 2005, **39**, (5), pp. 1291–1298
- [22] Wang C., Jiqng W., Zhou Y., Wang Y., Chen Z.: 'Synthesis of A-Fe ultrafine particles in a saturated salt solution/isopropanol/Pvp micro-emulsion and their structural characterization', *Mater. Res. Bull.*, 2000, **35**, (1), pp. 53–58
- [23] Liu T., Zhao L., Sun D., Tan X.: 'Entrapment of nanoscale zero-valent iron in chitosan beads for hexavalent chromium removal from wastewater', *J. Hazard. Mater.*, 2010, **184**, (1), pp. 724–730
- [24] Saleh N., Sirk K., Liu Y., *ET AL.*: 'Surface modifications enhance nanoiron transport and Napl targeting in saturated porous media', *Environ. Eng. Sci.*, 2007, **24**, (1), pp. 45–57
- [25] Pradhan N., Pal A., Pal T.: 'Silver nanoparticle catalyzed reduction of aromatic nitro compounds', *Colloids Surf. A*, 2002, **196**, (2), pp. 247–257
- [26] Chen Z., Wang T., Jin X., Chen Z., Megharaj M., Naidu R.: 'Multifunctional kaolinite-supported nanoscale zero-valent iron used for the adsorption and degradation of crystal violet in aqueous solution', *J. Colloid Interface Sci.*, 2013, **398**, pp. 59–66
- [27] Pootawang P., Lee S.Y.: 'Rapid synthesis of Ag nanoparticles-embedded mesoporous silica via solution plasma and its catalysis for 4-nitrophenol reduction', *Mater. Lett.*, 2012, **80**, pp. 1–4
- [28] Zhu Z., Guo X., Wu S., Zhang R., Wang J., Li L.: 'Preparation of nickel nanoparticles in spherical polyelectrolyte brush nanoreactor and their catalytic activity', *Ind. Eng. Chem. Res.*, 2011, **50**, (24), pp. 13848–13853
- [29] Rashid M.H., Mandal T.K.: 'Synthesis and catalytic application of nanostructured silver dendrites', *J. Phys. Chem. C*, 2007, **111**, (45), pp. 16750–16760
- [30] Jiang H.-L., Akita T., Ishida T., Haruta M., Xu Q.: 'Synergistic catalysis of Au@ Ag core-shell nanoparticles stabilized on metal-organic framework', *J. Am. Chem. Soc.*, 2011, **133**, (5), pp. 1304–1306
- [31] Aiello R., Sharp J., Matthews M.: 'Production of hydrogen from chemical hydrides via hydrolysis with steam', *Int. J. Hydrog. Energy*, 1999, **24**, (12), pp. 1123–1130
- [32] Shin K.S., Choi J.-Y., Park C.S., Jang H.J., Kim K.: 'Facile synthesis and catalytic application of silver-deposited magnetic nanoparticles', *Catal. Lett.*, 2009, **133**, (1–2), pp. 1–7
- [33] Kuroda K., Ishida T., Haruta M.: 'Reduction of 4-nitrophenol to 4-aminophenol over Au nanoparticles deposited on PMMA', *J. Mol. Catal. A, Chem.*, 2009, **298**, (1), pp. 7–11
- [34] Panigrahi S., Basu S., Praharaj S., *ET AL.*: 'Synthesis and size-selective catalysis by supported gold nanoparticles: study on heterogeneous and homogeneous catalytic process', *J. Phys. Chem. C*, 2007, **111**, (12), pp. 4596–4605
- [35] Jiang Z., Xie J., Jiang D., Jing J., Qin H.: 'Facile route fabrication of nano-Ni core mesoporous-silica shell particles with high catalytic activity towards 4-nitrophenol reduction', *Cryst. Eng. Commun.*, 2012, **14**, (14), pp. 4601–4611